

Spectral control of high harmonics from relativistic plasmas using bicircular fields

Zi-Yu Chen*

National Key Laboratory of Shock Wave and Detonation Physics, Institute of Fluid Physics,
China Academy of Engineering Physics, Mianyang 621999, China

(Dated: December 3, 2024)

We introduce two-color counterrotating circularly polarized laser fields as a new way to spectrally control high harmonic generation (HHG) from relativistic plasma mirrors. Through particle-in-cell simulations, we show only a selected group of harmonic orders can appear owing to the symmetry of the laser fields and the related conservation laws. By adjusting the intensity ratio of the two driving field components, we demonstrate the overall HHG efficiency, the relative intensity of allowed neighbouring harmonic orders, and the polarization state of the harmonic source can be tuned. The HHG efficiency of this scheme can be as high as driven by a linearly polarized laser field.

I. INTRODUCTION

High harmonic generation (HHG) from relativistically intense laser irradiating plasma surfaces is an extreme nonlinear process, which converts the fundamental driving laser frequency to its harmonics that can span thousands of harmonic orders[1–4]. One of the main mechanisms is the so called relativistically oscillating mirror (ROM) model[5–9]. The physical picture can be interpreted as relativistic Doppler up-shifting of the laser field reflected by the plasma surface which acts as a mirror oscillating with speed close to that of light. The harmonics are usually emitted in the form of a comb in the frequency domain and attosecond pulses in the time domain due to the broad spectral range. This thus provides a powerful radiation source in the extreme ultraviolet (XUV) and X-ray spectral region with attosecond duration. While many an investigation has been carried out to control the temporal structure of the harmonics, e.g., to obtain an isolated single attosecond pulse[10–13], methods to control the HHG spectrum remain limited. Among the reported spectral control schemes, selected enhancement of HHG has been achieved by modifying the plasma density ramp[14] or plasma surface morpha[15–19].

Here we consider controlling the harmonic spectrum by structuring the laser field. The approach is based on using circularly polarized (CP) two-color driving pulses rotating in opposite directions. Interestingly, it is known that the ROM HHG process is almost completely suppressed by using one single CP pulse at normal incidence[20], because the laser ponderomotive force in this case only contain slow-varying components following the pulse envelop. The situation may change drastically when combining two CP pulses with different frequency and helicity, as the pulses superposition can lead to very different field patterns as well as charge trajectories. It has already been shown both theoretically[21–24] and experimentally[25–27] that the bicircular configuration with one fundamental frequency ω and its counterrotating second harmonic 2ω can be effective in CP HHG from

atomic gases, whereas HHG process is also greatly suppressed driven by one-color CP pulse, due to electron's lateral spreading and reduced probability of re-collision with its parent ion. It is demonstrated that only specific sets of harmonic orders can be displayed and selectively enhanced in the harmonic spectrum driven by such bicircular fields[25–29]. However, applicability of extending this method from gas HHG to ROM HHG looks far from straightforward, since the underlying mechanisms between the two HHG scenarios are fundamentally different.

In this work, we show that bicircular fields can be used to control the spectrum of high harmonics from relativistic plasmas. Through numerical simulations, it is found that the harmonic spectral features, such as the appeared harmonic orders and their helicity, are governed by the symmetry of the laser fields and the related conservation laws. By breaking the rotational symmetry of the laser fields or the interaction geometry, the otherwise symmetry-forbidden frequencies can show up. By adjusting the relative intensity ratio of the bicircular driving fields, the harmonic spectral intensity can be modulated. The HHG process can have a high efficiency although using CP pulses and under normal incidence interactions.

II. SIMULATION SETUP

The simulations were performed using the one-dimensional (1D) particle-in-cell code VLPL (Virtual Laser Plasma Lab)[30]. The driving laser fields with fundamental frequency ω_0 (corresponding to wavelength $\lambda_0 = 800$ nm) and its second harmonic $2\omega_0$ are circularly polarized in the same plane but rotate in opposite directions:

$$\mathbf{E}(t) = \frac{1}{2i}(E_1 e^{i\omega_0 t} \hat{\mathbf{e}}_- + E_2 e^{2i\omega_0 t} \hat{\mathbf{e}}_+) + c.c., \quad (1)$$

where $\hat{\mathbf{e}}_{\pm} = (\hat{\mathbf{e}}_y \pm i\hat{\mathbf{e}}_z)/\sqrt{2}$ with $\hat{\mathbf{e}}_y$ and $\hat{\mathbf{e}}_z$ the unit vectors along y - and z -axis, respectively. The three-dimensional (3D) electric field waveform is shown in Fig. 1(a), where the intensity ratio of the two driving frequencies $I_{2\omega}/I_\omega = 0.5$ with $I_\omega = 2.8 \times 10^{21} \text{ W/cm}^2$

* ziyuch@caep.ac.cn

and $I_{2\omega} = 1.4 \times 10^{21} \text{ W/cm}^2$. The Lissajous figure projected in the $y - z$ polarization plane (in gray color) displays a characteristic feature of threefold spatio-temporal symmetry. The electric field experienced by the plasma electrons acts roughly as linearly polarized (LP) pulses rotated by 120° three times per optical cycle. This largely modified LP field pattern can give rise to harmonic emission as will be shown later. The temporal intensity profile has a Gaussian envelope with a full-width at half-maximum (FWHM) pulse duration of 30 fs. The laser pulse is normally incident onto a plasma target, of which the peak density is $n_0 = 200n_c$ and the thickness is 200 nm. Here $n_c = m_e\omega_0^2/4\pi e^2$ is the plasma critical density with respect to the fundamental laser frequency. An exponential density $n_e(x) = n_0 \exp(x/L_s)$ exists in the front surface of the plasma slab, where the preplasma scale length $L_s = 0.01\lambda_0$. The ions are taken to be immobile. The simulation cell size is $\lambda_0/1000$ and each cell is filled with 100 macroparticles. Absorption boundary condition is adopted for both fields and particles.

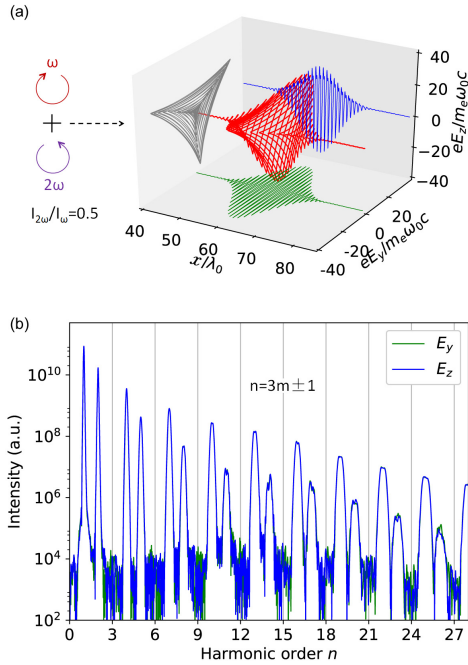


FIG. 1. (a) Electric field waveform of the incident laser pulses propagating along the x axis, composed of two-color (fundamental frequency and its second harmonic) counterrotating circularly polarized fields. (b) The corresponding high harmonic spectrum from surface plasmas.

III. RESULTS AND DISCUSSIONS

Figure 1(b) shows the harmonic spectra obtained by fast Fourier transform of the reflected electric field. It is clearly seen that only the harmonic orders with $n = 3m \pm 1$ ($m = 1, 2, 3, \dots$) have been generated, while ev-

ery third one with $n = 3m$ is missing. As the plasma is isotropic and the interaction is at normal incidence, this unique harmonic feature can be explained by the symmetry of the driving field as following. We follow the arguments of Kfir *et al*[27] and Pisanty *et al*[31]. The laser field vector, rotated by 120° per cycle in the polarization plane, satisfies,

$$\mathbf{E}^L(t + T_0/3) = \hat{R}_{(2\pi/3)} \mathbf{E}^L(t), \quad (2)$$

where $\hat{R}_{(2\pi/3)}$ is the 120° rotation operator. Assuming the emitted harmonic field conforms to the same dynamical symmetry and by taking Fourier transform, we can obtain the spectral field of the n th-order harmonic, $\mathbf{E}_n^{H_\omega}$, satisfying the following eigenvalue equation

$$e^{-2\pi in/3} \mathbf{E}_n^{H_\omega} = \hat{R}_{(2\pi/3)} \mathbf{E}_n^{H_\omega}. \quad (3)$$

The solutions are (i) $n = 3m + 1$, so that $e^{-2\pi in/3} \mathbf{E}_n^{H_\omega} = e^{-2\pi i/3} \mathbf{E}_n^{H_\omega}$ and (ii) $n = 3m - 1$, so that $e^{-2\pi in/3} \mathbf{E}_n^{H_\omega} = e^{+2\pi i/3} \mathbf{E}_n^{H_\omega}$. Apart from these two sets of harmonic orders, the harmonic orders with $n = 3m$ do not satisfy Eq. (3) and are therefore forbidden by the threefold symmetry.

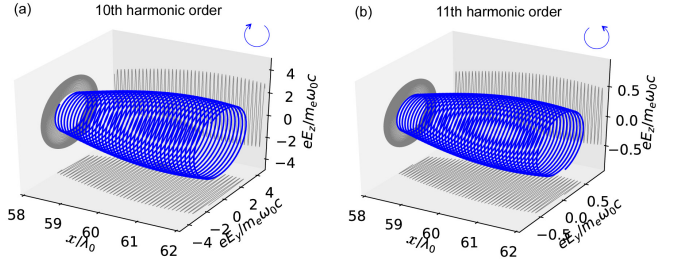


FIG. 2. Electric field waveform of the (a) 10th and (b) 11th harmonic shown in Fig. 1(b). In order to see the helicity clearly, only parts of the waveform are shown. The rotation direction is defined as seen by a wave receiver and the harmonic waves propagate along the $-x$ axis.

The preceding selection rules are also consistent with the conservation laws for energy, parity and spin angular momentum[26, 31]. Considering the HHG process in a simple photon-exchange picture, conservation of energy implies each harmonic frequency can be expressed in the form of

$$\Omega_{(n_1, n_2)}^H = n_1 \cdot \omega_0 + n_2 \cdot 2\omega_0, \quad (4)$$

where n_1 and n_2 are integers. Applying parity operation on both the incoming and outgoing photons, we have

$$P[h_{(\Omega_{(n_1, n_2)}^H)}] = -1; \quad (5)$$

$$P[h_{(n_1 \cdot \omega_0; n_2 \cdot 2\omega_0)}] = (-1)^{n_1 + n_2}, \quad (6)$$

where P is parity and h represents helicity. Conservation of parity requires that $n_1 + n_2$ must be odd. In addition, conservation of spin angular momentum leads to

$$\sigma_{(n_1, n_2)}^H = n_1 \sigma_1 + n_2 \sigma_2. \quad (7)$$

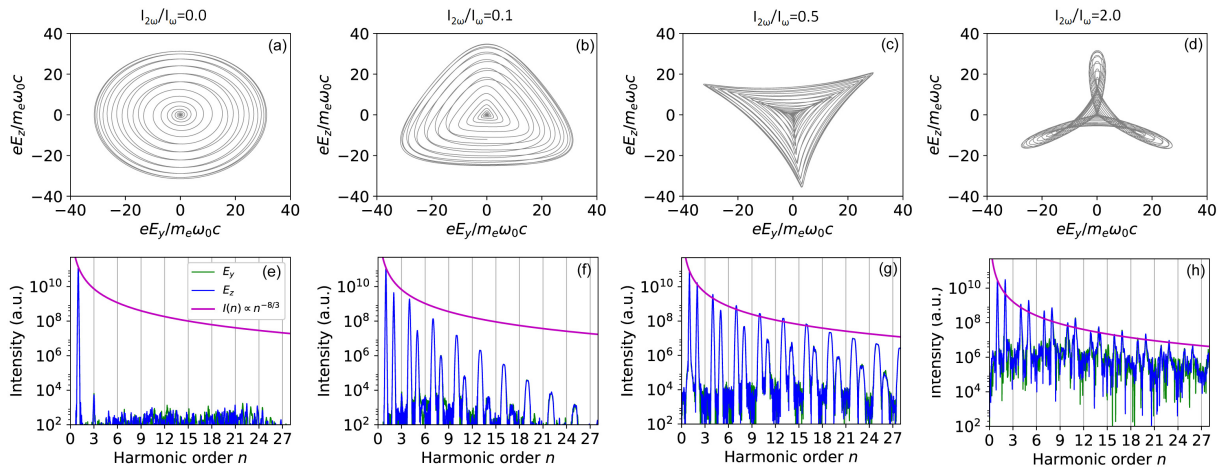


FIG. 3. Polarization plane projections of the laser electric fields generated with intensity ratios (a) $I_{2\omega}/I_\omega = 0.0$, (b) $I_{2\omega}/I_\omega = 0.1$, (c) $I_{2\omega}/I_\omega = 0.5$, and (d) $I_{2\omega}/I_\omega = 2.0$. The total intensity is kept constant ($I_\omega + I_{2\omega} = 4.2 \times 10^{21} \text{ W/cm}^2$). (e)-(h) The generated harmonic spectra corresponding to the lasers of panel (a)-(d).

Since the ω_0 and $2\omega_0$ driving pulses are counterrotating, we can set $\sigma_1 = 1, \sigma_2 = -1$. For photon spin, $-1 \leq \sigma_{(n_1, n_2)} \leq 1$. Then it is easily seen that $n_2 - 1 \leq n_1 \leq n_2 + 1$, which together with the parity requirement means that n_1 and n_2 must differ by unity. Therefore, only two cases are allowed, i.e., (i) $n_1 = m+1$ and $n_2 = m$, leading to $(m+1)\omega_0 + m \cdot 2\omega_0 = (3m+1)\omega_0$; (ii) $n_1 = m$ and $n_2 = m+1$, leading to $m\omega_0 + (m+1) \cdot 2\omega_0 = (3m+2)\omega_0$. Note $3m+2$ is equivalent to $3m-1$. These two selection rules also indicate that the $n = 3m+1$ harmonic orders have the same helicity with the fundamental field, while the $n = 3m+2$ orders co-rotate with the $2\omega_0$ field. These are consistent with the eigenvalues $e^{-2\pi i/3}$ and $e^{+2\pi i/3}$ of Eqs. (3), which also imply the $n = 3m+1$ and $n = 3m-1$ harmonics have opposite helicity.

The aforementioned harmonic helicity is confirmed by the simulation results. Figure 2 shows the 3D electric field waveform of a representative group of neighbouring harmonics ($n = 10$ and $n = 11$). To see the helicity clearly, only parts of the waveform are shown. Each harmonic is circularly polarized. The helicity of the 10th harmonic is the same as the fundamental field, while the 11th harmonic is the same as the second harmonic field. The other harmonic groups share the same features. We note although the adjacent harmonics have alternating helicity, the relative intensity of neighbouring harmonics is not equal (see Fig. 1(b)). Here the $n = 3m+2$ harmonics are weaker than the $n = 3m+1$ harmonics, due to the $2\omega_0$ field less intense than the ω_0 field. As a result, harmonics of all the groups combined can be circularly or elliptically polarized. Otherwise, the combined harmonic fields should be close to linear polarization[32]. This offers a new way to generate CP HHG and attosecond pulses from relativistic plasmas[33, 34]. Such radiation sources can find important applications in ultrafast measurement of chiral molecules[35] and magnetic materials[36].

Next, we show the harmonic intensity can be modulated by adjusting the intensity ratio of the two driving pulses. We keep the total intensity of the two fields constant ($I_\omega + I_{2\omega} = 4.2 \times 10^{21} \text{ W/cm}^2$) as the ratio $I_{2\omega}/I_\omega$ varies from 0 to 0.1, 0.5, and 2. The remaining parameters are the same as in Fig. 1. The Lissajous figures of the superposed electric fields are displayed in Figs. 3(a)-(d). The corresponding harmonic spectra are shown in Figs. 3(e)-(h). For the case of $I_{2\omega}/I_\omega = 0$, i.e., one-color CP driving laser only, high harmonics with orders $n > 3$ are indeed strongly suppressed, almost at the noise level. As the laser intensity ratio is increased, the harmonic intensity is significantly enhanced. For $I_{2\omega}/I_\omega = 2.0$, the spectral intensity of all the allowed harmonic orders is close to the $I(n) \propto n^{-8/3}$ scaling, which is theoretically derived for the case of LP driving lasers[7] and already confirmed by experimental results[9]. This indicates the scheme of bicircular driving lasers can also be very efficient in high harmonic generation. The enhancement of HHG efficiency can be attributed to the different field vector pattern induced by different laser intensity ratio. As the laser field experienced by the plasma electrons gets closer to linearly polarized, stronger harmonic strength can be expected. Besides, as increasing $I_{2\omega}$, the relative intensity of allowed neighbouring harmonic orders I_{3m+2}/I_{3m+1} also increases. This would change the overall polarization state of the harmonic source.

Although the Lissajous figures in Figs. 3(b)-(d) have a very different appearance, they all keep a threefold symmetry. Therefore, the harmonic spectra in Figs. 3(f)-(h) have the same selection rule as $n = 3m \pm 1$. When the threefold symmetry is lost, the selection rule described above on longer holds. A variety of harmonic channels can open up. The simplest way to break the threefold rotational symmetry of the interaction is to change the incidence geometry from normal to oblique. In the oblique incidence case, the symmetry breaking can be seen more

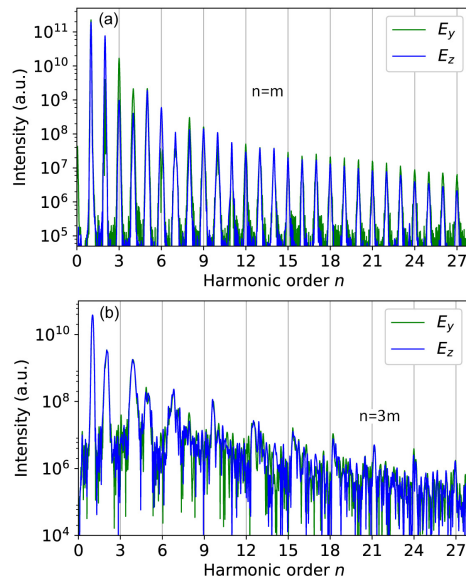


FIG. 4. High harmonic spectrum for the case of (a) oblique incidence with incidence angle $\theta = 45^\circ$ and (b) plasma scale length of $L_s = 0.15\lambda_0$. The other simulation parameters are the same as in Fig. 1.

clearly by considering the interaction in the 1D case. Using Bourdier's method to take Lorentz transformations from the laboratory frame to a moving frame[37], the laser pulse can be transformed to be at normal incidence (wave vector $\mathbf{k} = k\hat{\mathbf{e}}_x$). At the same time, the plasmas initially stream along the $-\hat{\mathbf{e}}_y$ direction while are stationary along the $\hat{\mathbf{e}}_z$ direction. Thus the rotational symmetry in the $(y-z)$ polarization plane is broken. Consequently, the previously symmetry-forbidden $n = 3m$ orders can appear. Figure 4(a) shows the bicircular field-driven harmonic spectrum for the case of oblique incidence with incidence angle $\theta = 45^\circ$. The other simulation parameters are the same as in Fig. 1. We see the harmonic orders with $n = 3m$ are indeed shown in this case.

It is interesting to note only the $n = 3m$ harmonic orders appear in the spectrum for $n > 15$ shown in Fig. 4(b), where the plasma scale length $L_s = 0.15$ while the other simulation parameters are the same as in Fig. 1. The physical origin for this "abnormal" phenomena, however, is not from symmetry-based selection rules, but more likely from plasma effects. On the one

hand, the appearance of $n = 3m + 1$ and $n = 3m + 2$ orders and the absence of $n = 3m$ orders for $n < 10$ reflect the preservation of the threefold symmetry. On the other hand, as L_s becomes longer, significant plasma waves can be excited and are able to couple to the incident wave. Consequently, various parametric instabilities and self-phase modulation effects[38], together with chirp effect due to motion of surface plasmas[39], can result in harmonic spectral modulation, splitting and frequency shifting. The gradual frequency shifting from the $n = 3m + 1$ orders to match the $n = 3m$ orders is evident when the harmonics of $n > 12$ are compared. The absence of the $n = 3m + 2$ orders in this case may be explained as too weak to distinguish. For even longer L_s , however, the whole high harmonic structure would disappear due to strong plasma modulation effects and low efficiency of the ROM mechanism in this case.

IV. CONCLUSIONS

In summary, we have introduced bicircular counter-rotating two-color fields to HHG in the relativistic plasma regime. We numerically demonstrate, by adjusting the intensity ratio of the two driving fields, the properties of the high harmonics, including the allowed harmonic orders, their overall intensity, the relative intensity of allowed neighbouring harmonic orders, as well as the polarization state of the harmonics, can be controlled. The underlying mechanisms can be understood as a result of symmetry effect and related conservation laws. This scheme opens up more possibilities in controlling the surface harmonics, as more degrees of freedom can be adjusted, such as the frequency, ellipticity, and relative phase of the two drivers in the counterrotating two-color fields.

ACKNOWLEDGMENTS

This work was supported in part by the National Nature Science Foundation of China (Grant Nos. 11505172 and 11705185) and the Presidential Fund of China Academy of Engineering Physics (Grant No. YZJJLX2017002).

[1] U. Teubner and P. Gibbon, "High-order harmonics from laser-irradiated plasma surfaces," *Rev. Mod. Phys.* **81**, 445–479 (2009).
[2] S. Gordienko, A. Pukhov, O. Shorokhov, and T. Baeva, "Relativistic Doppler effect: universal spectra and zep-to-second pulses," *Phys. Rev. Lett.* **93**, 115002 (2004).
[3] S. Gordienko, A. Pukhov, O. Shorokhov, and T. Baeva, "Coherent focusing of high harmonics: a new way to

wards the extreme intensities," *Phys. Rev. Lett.* **94**, 103903 (2005).
[4] B. Dromey, S. Kar, C. Bellei, D. C. Carroll, R. J. Clarke, J. S. Green, S. Kneip, K. Markey, S. R. Nagel, P. T. Simpson, L. Willingale, P. McKenna, D. Neely, Z. Na-jmudin, K. Krushelnick, P. A. Norreys, and M. Zepf, "Bright multi-keV harmonic generation from relativistically oscillating plasma surfaces," *Phys. Rev. Lett.* **99**,

085001 (2007).

[5] S. V. Bulanov, N. M. Naumova, and F. Pegoraro, "Interaction of an ultrashort, relativistically strong laser pulse with an overdense plasma," *Phys. Plasmas* **1**, 745 (1994).

[6] R. Lichters, J. Meyer-ter-Vehn, and A. Pukhov, "Short-pulse laser harmonics from oscillating plasma surfaces driven at relativistic intensity," *Phys. Plasmas* **3**, 3425 (1996).

[7] T. Baeva, S. Gordienko, and A. Pukhov, "Theory of high-order harmonic generation in relativistic laser interaction with overdense plasma," *Phys. Rev. E* **74**, 046404 (2006).

[8] A. Pukhov, "Relativistic plasmas: X-rays in a flash," *Nat. Phys.* **2**, 439-440 (2006).

[9] B. Dromey, M. Zepf, A. Gopal, K. Lancaster, M. S. Wei, K. Krushelnick, M. Tatarakis, N. Vakakis, S. Mousaizis, R. Kodama, M. Tampo, C. Stoeckl, R. Clarke, H. Habara, D. Neely, S. Karsch, and P. Norreys, "High harmonic generation in the relativistic limit," *Nat. Phys.* **2**, 456-459 (2006).

[10] T. Baeva, S. Gordienko, and A. Pukhov, "Relativistic plasma control for single attosecond x-ray burst generation," *Phys. Rev. E* **74**, 065401(R) (2006).

[11] S. G. Rykov, M. Geissler, J. Meyer-ter-Vehn, G. D. Tsakiris, "Intense single attosecond pulses from surface harmonics using the polarization gating technique," *New J. Phys.* **10**, 025025 (2008).

[12] L. Liu, C. Xia, J. Liu, W. Wang, Y. Cai, C. Wang, R. Li, and Z. Xu, "Control of single attosecond pulse generation from the reflection of a synthesized relativistic laser pulse on a solid surface" *Phys. Plasmas* **15**, 103107 (2008).

[13] F. Cambronero-López, M. Blanco, C. Ruiz, M. T. Flores-Arias, and C. Bao-Varela, "Polarization gating using cross-polarized wave generation with multicycle lasers to produce isolated attosecond pulses in overdense media" *J. Opt. Soc. Am. B* **34**, 843-849 (2017).

[14] B. Dromey, S. G. Rykov, D. Adams, R. Hörlein, Y. Nomura, D. C. Carroll, P. S. Foster, S. Kar, K. Markey, P. McKenna, D. Neely, M. Geissler, G. D. Tsakiris, and M. Zepf, "Tunable enhancement of high harmonic emission from laser solid interactions," *Phys. Rev. Lett.* **102**, 225002 (2009).

[15] X. Lavocat-Dubuis and J. P. Matte, "Numerical simulation of harmonic generation by relativistic laser interaction with a grating," *Phys. Rev. E* **80**, 055401 (2009).

[16] X. Lavocat-Dubuis and J. P. Matte, "Numerical and theoretical study of the generation of extreme ultraviolet radiation by relativistic laser interaction with a grating," *Phys. Plasmas* **17**, 093105 (2010).

[17] M. Cerchez, A. L. Giesecke, C. Peth, M. Toncian, B. Albertazzi, J. Fuchs, O. Willi, and T. Toncian, "Generation of laser-driven higher harmonics from grating targets," *Phys. Rev. Lett.* **110**, 065003 (2013).

[18] L. Fedeli, A. Sgattoni, G. Cantono, and A. Macchi, "Relativistic surface plasmon enhanced harmonic generation from gratings," *Appl. Phys. Lett.* **110**, 051103 (2017).

[19] G. Zhang, M. Chen, F. Liu, X. Yuan, S. Weng, J. Zheng, Y. Ma, F. Shao, Z. Sheng, and J. Zhang, "Directional enhancement of selected high-order-harmonics from intense laser irradiated blazed grating targets," *Opt. Express* **25**, 23567-23578 (2017).

[20] M. Yeung, B. Dromey, S. Cousens, T. Dzelzainis, D. Kiefer, J. Schreiber, J. H. Bin, W. Ma, C. Kreuzer, J. Meyer-ter-Vehn, M. J. V. Streeter, P. S. Foster, S. Rykov, and M. Zepf, "Dependence of laser-driven coherent synchrotron emission efficiency on pulse ellipticity and implications for polarization gating," *Phys. Rev. Lett.* **112**, 123902 (2014).

[21] S. Long, W. Becker, and J. K. McIver, "Model calculations of polarization-dependent two-color high-harmonic generation," *Phys. Rev. A* **52**, 2262 (1995).

[22] W. Becker, B. N. Chichkov, and B. Wellegehausen, "Schemes for the generation of circularly polarized high-order harmonics by two-color mixing," *Phys. Rev. A* **60**, 1721 (1999).

[23] D. B. Milošević, W. Becker, and R. Kopold, "Generation of circularly polarized high-order harmonics by two-color coplanar field mixing," *Phys. Rev. A* **61**, 063403 (2000).

[24] L. Medišauskas, J. Wragg, H. van der Hart, and M. Y. Ivanov, "Generating elliptically polarized attosecond pulses using bichromatic counterrotating circularly polarized laser fields," *Phys. Rev. Lett.* **115**, 153001 (2015).

[25] H. Eichmann, A. Egbert, S. Nolte, C. Momma, B. Wellegehausen, W. Becker, S. Long, and J. K. McIver, "Polarization-dependent high-order two-color mixing," *Phys. Rev. A* **51**, 3414(R) (1995).

[26] A. Fleischer, O. Kfir, T. Diskin, P. Sidorenko, and O. Cohen, "Spin angular momentum and tunable polarization in high harmonic generation," *Nat. Photonics* **8**, 543 (2014).

[27] O. Kfir, P. Grychtol, E. Turgut, R. Knut, D. Zusin, D. Popmintchev, T. Popmintchev, H. Nembach, J. M. Shaw, A. Fleischer, H. Kapteyn, M. Murnane, and O. Cohen, "Generation of bright phase-matched circularly polarized extreme ultraviolet high harmonics," *Nat. Photonics* **9**, 99 (2015).

[28] D. Baykusheva, M. S. Ahsan, N. Lin, and H. J. Wörner, "Bicircular high-harmonic spectroscopy reveals dynamical symmetries of atoms and molecules," *Phys. Rev. Lett.* **116**, 123001 (2016).

[29] K. M. Dorney, J. L. Ellis, C. Hernández-García, D. D. Hickstein, C. A. Mancuso, N. Brooks, T. Fan, G. Fan, D. Zusin, C. Gentry, P. Grychtol, H. C. Kapteyn, and M. M. Murnane, "Helicity-selective enhancement and polarization control of attosecond high harmonic waveforms driven by bichromatic circularly polarized laser fields," *Phys. Rev. Lett.* **119**, 063201 (2017).

[30] A. Pukhov, "Three-dimensional electromagnetic relativistic particle-in-cell code VLPL (Virtual Laser Plasma Lab)," *J. Plasma Phys.* **61**, 425 (1999).

[31] E. Pisanty, S. Sukiasyan, and M. Ivanov, "Spin conservation in high-order-harmonic generation using bicircular fields," *Phys. Rev. A* **90**, 043829 (2014).

[32] D. B. Milošević and W. Becker, "Attosecond pulse trains with unusual nonlinear polarization," *Phys. Rev. A* **62**, 011403(R) (2000).

[33] Z.-Y. Chen and A. Pukhov, "Bright high-order harmonic generation with controllable polarization from a relativistic plasma mirror," *Nat. Commun.* **7**, 12515 (2016).

[34] G. Ma, W. Yu, M. Y. Yu, B. Shen, and L. Veisz, "Intense circularly polarized attosecond pulse generation from relativistic laser plasmas using few-cycle laser pulses," *Opt. Express* **24**, 10057 (2016).

[35] R. Cireasa, A. E. Boguslavskiy, B. Pons, M. C. H. Wong, D. Descamps, S. Petit, H. Ruf, N. Thiré, A. Ferré, J. Suarez, J. Higuet, B. E. Schmidt, A. F. Alharbi, F. Légaré, V. Blanchet, B. Fabre, S. Patchkovskii, O. Smirnova, Y. Mairesse, and V. R. Bhardwaj, "Probing molecular chirality on a sub-femtosecond timescale," *Nat.*

Phys. **11**, 654-658 (2015).

[36] F. Willems, C. T. L. Smeenk, N. Zhavoronkov, O. Kornilov, I. Radu, M. Schmidbauer, M. Hanke, C. von Korff Schmising, M. J. J. Vrakking, and S. Eisebitt, "Probing ultrafast spin dynamics with high-harmonic magnetic circular dichroism spectroscopy," Phys. Rev. B **92**, 220405(R) (2015).

[37] A. Bourdier, "Oblique incidence of a strong electromagnetic wave on a cold inhomogeneous electron plasma. Relativistic effects," Phys. Fluids **26**, 1804 (1983).

[38] F. Dollar, P. Cummings, V. Chvykov, L. Willingale, M. Vargas, V. Yanovsky, C. Zulick, A. Maksimchuk, A. G. R. Thomas, and K. Krushelnick, "Scaling high-order harmonic generation from laser-solid interactions to ultra-high intensity," Phys. Rev. Lett. **110**, 175002 (2013).

[39] M. Behmke, D. an der Brügge, C. Rödel, M. Cerchez, D. Hemmers, M. Heyer, O. Jäckel, M. Kübel, G. G. Paulus, G. Pretzler, A. Pukhov, M. Toncian, T. Toncian, and O. Willi, "Controlling the spacing of attosecond pulse trains from relativistic surface plasmas," Phys. Rev. Lett. **106**, 185002 (2011).